ACS Sustainable Chemistry & Engineering

Research Article

pubs.acs.org/journal/ascecg

Preparation of Superoleophobic and Superhydrophobic Titanium Surfaces via an Environmentally Friendly Electrochemical Etching Method

Yao Lu, Jinlong Song, Xin Liu, Wenji Xu,* Yingjie Xing, and Zefei Wei

School of Mechanical Engineering, Dalian University of Technology, Dalian 116024, People's Republic of China

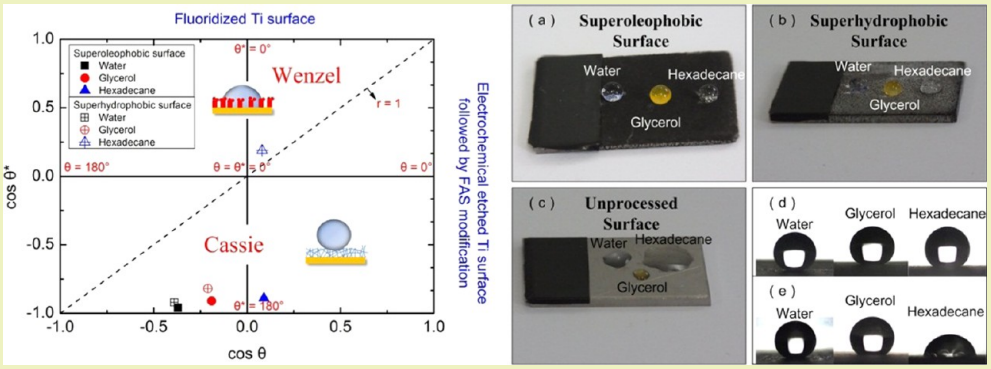

ABSTRACT: The preparation of superoleophobic and superhydrophobic surfaces requires surface microgeometries and surface chemistry. In this study, an economical and environmentally friendly electrochemical etching method was developed to prepare superoleophobic and superhydrophobic titanium surfaces. Scanning electron microscopy (SEM), X-ray diffraction (XRD), Fourier transform infrared spectrophotometry (FTIR), energy-dispersive spectroscopy (EDS), and optical contact angle measurements were used to characterize the surface morphologies, crystal structures, chemical compositions, and wettability of the surfaces for both water and oil. The results show that the prepared superoleophobic surface has water, glycerol, and hexadecane contact angles above 150°, with rolling angles of only 1−2°. Analysis of the electrolyte, the reaction process, and the products demonstrates that the proposed method is inexpensive and environmentally friendly. The effects of electrochemical parameters such as current density, electrochemical etching time, electrolyte temperature, and electrolyte concentration on the surface wettability for water, glycerol, and hexadecane were also investigated. Superoleophobicity and superhydrophobicity can be selectively obtained by varying the electrochemical parameters. The proposed method is believed to be adopted for industrial production of superoleophobic and superhydrophobic titanium surfaces.

KEYWORDS: *Superoleophobic, Superhydrophobic, Electrochemical etching, Titanium surfaces, Environmentally friendly*

INTRODUCTION

Many natural surfaces are superhydrophobic, including various plant leaves and the legs of a water strider.[1−3] These surfaces exhibit water contact angles (surface tension γ_w = 72.1 mN/m) greater than 150°. Lotus effect is the best-known property of superhydrophobic surfaces in self-cleaning. This effect is due to a combination of surface chemistry and rough micro/nanometer structures. However, liquids with lower surface tensions, such as hexadecane (γ_h = 27.5 mN/m), rapidly spread across the lotus leaf, leading to a contact angle of nearly 0°. In addition, the oleophilicity may lead to the loss of the self-cleaning ability of superhydrophobic surfaces in polluted water.[4] Thus, superoleophobic surfaces with liquid (whose surface tension is lower than that of water) contact angles greater than 150° as well as low rolling angles have considerable potential values in fundamental research and industrial applications, such as in understanding the wetting behavior,[5] oil transfer, and self-cleaning in oily conditions. Surfaces that are oil-repellent in air are scarcely found in nature.[6] Thus, artificial superoleophobic surfaces have attracted considerable scientific attention worldwide.

Nowadays, numerous studies on superhydrophobic surface preparation have been reported.[7−14] However, compared with superhydrophobicity, superoleophobicity is significantly more difficult and complicated to achieve because of the low surface tension of liquids.[15,16]

Three models were developed by Young,[17] Wenzel,[18] and Cassie and Baxter,[19] respectively. The Young model (Scheme 1a) describes the contact angle of a droplet on a smooth surface according to the expression:

$$\cos\theta = (\gamma_{sv} - \gamma_{sl})/\gamma_{lv} \quad (1)$$

where θ is the liquid contact angle on a smooth surface, γ is the interfacial tension, and the subscripts s, v, and l refer to the

Received: July 15, 2012
Revised: September 21, 2012
Published: October 15, 2012

   dx.doi.org/10.1021/sc3000527 | ACS Sustainable Chem. Eng. 2013, 1, 102−109

Scheme 1. (a) Young Model, (b) Wenzel Model, and (c) Cassie and Baxter Model

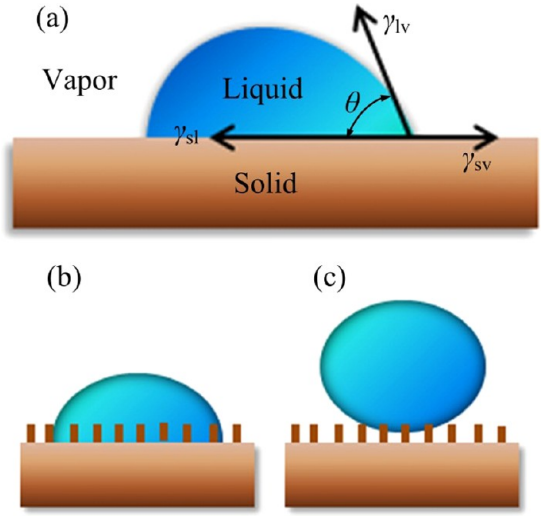

solid, vapor, and liquid phases, respectively. In consideration of the effect of surface roughness, Wenzel and Cassie developed their models based on Young's model. Wenzel believed the available solid surface area is increased by surface roughness; thus, the Wenzel model (Scheme 1b) describes the surface contact angle according to the equation:

$$\cos\theta^* = r\cos\theta \quad (2)$$

where θ^* refers to the apparent contact angle on the textured surface, r refers to the surface roughness, and θ is the contact angle given by Young's model. On the other hand, the Cassie and Baxter model recognizes that the hydrophobicity of a rough surface is due to micronanometer-scale pockets of air trapped under the liquid droplet, leading to a composite interface.[4] The Cassie and Baxter (Scheme 1c) equation is written as

$$\cos\theta^* = -1 + \varphi_s(1 + \cos\theta) \quad (3)$$

where φ_s is the fraction of the solid in contact with the liquid.

It can be deduced from eqs 1, 2, and 3 that θ^* is becoming smaller as the liquid surface tension in air γ_{lv} gets smaller (other parameters do not change). Thus, contact angles larger than 150° for low surface tension liquids are more demanding.

To date, some methods are used to fabricate superoleophobic surfaces. Tuteja and co-workers[4,20,21] designed superolephobic surfaces via electrospun method and first proposed the importance of re-entrant geometries on superoleophobic surfaces. Guittard and co-workers[22,23] successfully

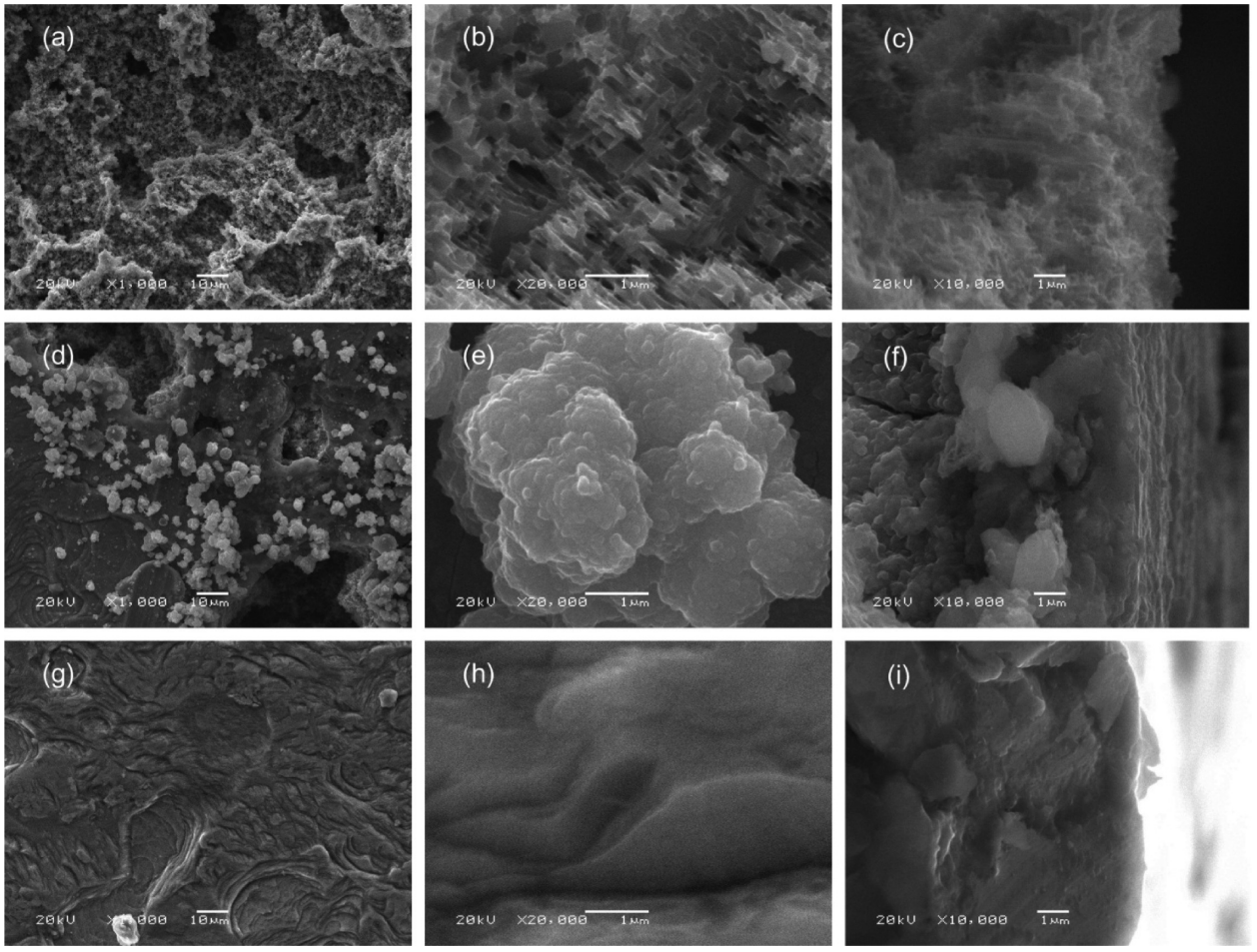

Figure 1. SEM images of (a–c) superoleophobic Ti surface electrochemically etched for 10 min in 0.2 mol L^{-1} NaBr solution at a 1.0 A/cm^2 current density and at 60–70 °C electrolyte temperature; (d–f) superhydrophobic Ti surface electrochemically etched for 10 min in 0.2 mol L^{-1} NaBr solution at a 0.25 A/cm^2 current density and at 60–70 °C electrolyte temperature; and (g–i) unprocessed Ti surface. (c), (f), and (i) are the flank of superoleophobic Ti surface, superhydrophobic Ti surface, and unprocessed Ti surface, respectively.

dx.doi.org/10.1021/sc3000527 | ACS Sustainable Chem. Eng. 2013, 1, 102–109

prepared superoleophobic surfaces via electrodeposition. Tian et al.[24] reported the preparation of superolephobic surfaces through the electrochemical growth of gold pyramidal nanostructures. However, superoleophobic surface preparation via electrochemical etching has been rarely reported. In the present work, a simple electrochemical etching method was used to prepare superoleophobic titanium (Ti) surfaces using a neutral, environmentally friendly, and low-cost NaBr solution. The electrochemical parameters, including the electrochemical etching time, current density, electrolyte temperature, and electrolyte concentration, were also studied. These parameters determine the surface microstructures that affect the hydrophobicity or oleophobicity. Here, the electrochemical method is a process to remove materials selectively by electrochemical reaction at the anode in an electrolytic cell.[25] Therefore, we used this easily controlled method so that it can meet the requirements of different parameters.

EXPERIMENTAL SECTION

Specimen Preparation. The Ti specimens (20 mm × 20 mm × 2 mm, SUNTEC Titanium LTD, Dalian) were used as anodes, whereas a copper plate of the same size as the Ti specimens was used as the cathode. Both electrodes were placed in a 0.1−1.0 mol L^{-1} NaBr solution and positioned face-to-face at a distance of 10 mm. Electrochemical etching was performed under magnetic stirring from 1 to 15 min at a current density of 0.125 to 1.25 A/cm^2 and at an electrolyte temperature of 30−80 °C.

The specimens were then ultrasonically rinsed with deionized water and subsequently dried. The Ti specimens were then immersed in a 1.0 wt % ethanol solution of fluoroalkylsilane [FAS, $C_8F_{13}H_4Si(OCH_2CH_3)_3$, a low surface energy material, Degussa Co., Germany] for 2 h and then heated at 80 °C for 15 min. In this experiment, all chemicals were of analytical grade. Superhydrophobic and superoleophobic Ti surfaces were then obtained under certain electrochemical parameters.

Specimen Characterization. The surface morphologies of the specimens were observed under a scanning electron microscope (SEM, JSM-6360LV, Japan). The crystal structures of the specimens were examined using an X-ray diffractometer (XRD-6000, Japan). The X-ray source was a Cu Kα radiation (λ = 0.15418 nm), which was operated at 40 kV and 40 mA within the 30° and 100° range, at a scanning rate of 2θ = 0.026°/min. The surface chemical compositions were investigated using a Fourier-transform infrared spectrophotometer (FTIR, JASCO, Japan) and an energy-dispersive spectrometer (EDS, INCA Energy, Oxford 135Ins, Japan). The contact and rolling angles were measured at ambient temperature via the sessile-drop method using an optical contact angle meter (DSA100, Krüss, Germany). Water droplets (5 μL) were carefully dropped onto specimen surfaces, and the average of five measurements obtained at different positions in the specimens was adopted as the final contact angle.

RESULTS AND DISCUSSION

Surface Characterization. The superhydrophobic surfaces display rough micro/nanometer surface morphologies, however, the superoleophobic surfaces show re-entrant geometries.[4] Figure 1a−c shows the SEM images of a superoleophobic Ti surface electrochemically etched for 10 min in a 0.2 mol L^{-1} NaBr solution at a 1.0 A/cm^2 current density and at 60−70 °C electrolyte temperature. Figure 1a shows that the processed superoleophobic Ti surface has numerous micrometer-scale protrusions and pores resulting from electrochemical etching. On the other hand, Figure 1b shows the nanometer-scale needle-like structures, the width of which varied from 50 to 300 nm, on the Ti surface. Figure 1c shows the flank of the processed superoleophobic Ti surface. The textured Ti surface exhibited the re-entrant geometries that are the key to achieving oleophobicity.[4,15] Figure 1d−f shows the SEM images of a superhydrophobic Ti surface electrochemically etched for 10 min in the 0.2 mol L^{-1} NaBr solution at a 0.25 A/cm^2 current density and at 60−70 °C electrolyte temperature. Several mastoids, ranging in size from 3 to 5 μm, are found on the surface (Figure 1d), and the etching was not as complete or as even as that of the superoleophobic Ti surface (Figure 1a). Nanoflakes ranging in size from 100 to 500 nm were present on the Ti surface (Figure 1e). These nanometer-scale structures are necessary in superhydrophobic surfaces.[26] However, given the lack of re-entrant structures (Figure 1f), the Ti surface was not oleophobic. Figure 1g−i shows the SEM images of an unprocessed Ti surface. Only a few crevices and gaps were on the surface, without any nanometer-scale structures. Thus, the lack of rough micro/nanometer structures made the unprocessed Ti surface neither hydrophobic nor oleophobic.

The surface crystal structures were analyzed via XRD. Figure 2 shows the XRD patterns of the superoleophobic Ti surface, superhydrophobic Ti surface, and the unprocessed Ti surface. In the 2θ scan range of 30−100°, the superoleophobic Ti surface, superhydrophobic Ti surface, and unprocessed Ti surface all show characteristic peaks of Ti(100), Ti(002), Ti(101), Ti(102), Ti(110), Ti(103), Ti(112), Ti(201), Ti(004), and Ti(104) at 35.02°, 38.32°, 40.10°, 52.92°, 62.90°, 70.58°, 76.12°, 77.32°, 82.20°, and 92.66°, respectively. These data are in good agreement with the Ti crystallographic data (JCPDS card no. 44-1294). The 10 peaks are due to the formation of Ti oxides (TiO_2/Ti_7O_{13}/Ti_9O_{17}, whose JCPDS card numbers are 53-0619, 50-0789, and 50-0791, respectively) in the crystalline phase. No significant difference was found between the superoleophobic Ti surface, the superhydrophobic Ti surface, and the unprocessed Ti surface. Therefore, the presence of crystal structures is not a factor in the hydrophobicity or oleophobicity of the surfaces.

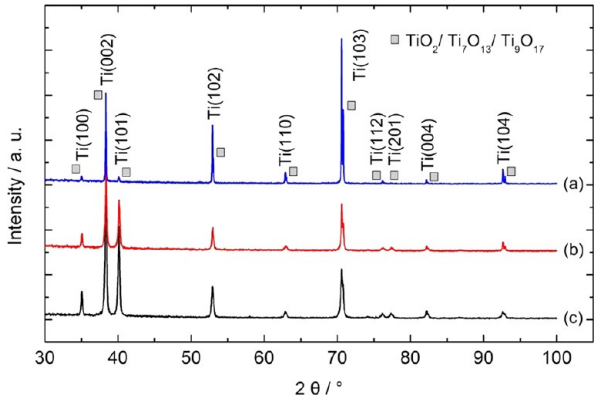

Figure 2. XRD patterns of (a) superoleophobic Ti surface, (b) superhydrophobic Ti surface, and (c) unprocessed Ti surface.

SEM and XRD results reveal that the generation of the re-entrant geometries and nanoflakes can be explained by the theories of Kelly[27] and Noël.[28] The reactions occurred both

dx.doi.org/10.1021/sc3000527 | ACS Sustainable Chem. Eng. 2013, 1, 102−109

inside and outside the crevices and gaps in the Ti surfaces. Ti oxidation was followed by Ti^{4+} hydrolysis according to the following equation:

$$Ti^{4+} + 4H_2O \rightarrow Ti(OH)_4 \downarrow + 4H^+ \quad (4)$$

Acidification occurred within the crevice as a result of H^+ production. At the same time, oxygen reduction occurred on the passive exterior of the Ti surface of a corroding crevice, and OH^- was formed in the neutral NaBr solution according to the following reaction:

$$O_2 + 2H_2O + 4e^- \rightarrow 4OH^- \quad (5)$$

H^+ was then consumed as follows:

$$2H^+ + 2e^- \rightarrow H_2\uparrow \quad (6)$$

and

$$H^+ + e^- \rightarrow H \quad (7)$$

H_2 was produced from the solution, and the hydrogen atom was then absorbed into the Ti matrix. The amounts of proton produced and consumed by these reactions are equivalent. Therefore, the proton reduction reaction could induce Ti dissolution without affecting the pH. During the reaction, the solution remained neutral, thus causing less environmental harm than an acid or alkali solution. The NaBr solution was inexpensive and neutral, thus making it highly economical and environmentally friendly. In terms of the reaction products, H_2 and $Ti(OH)_4$ are comparatively harmless. As the process continued, rough micro/nanometer structures were gradually created. By adjusting the process parameters, re-entrant geometries or nanoflakes could be selectively obtained, thus resulting in different surface oleophobicities or hydrophobicities after low surface energy material modifications.

Superoleophobic surfaces are similar to superhydrophobic surfaces in that these materials also require low surface energy material modifications. The surface chemical compositions were investigated via FTIR. The FTIR spectrum of the superoleophobic Ti surface, which had been modified by FAS, shows absorption bands at 1399.93, 1239.72, 1210.46, 1144.81, 1120.13, and 1068.79 cm^{-1} (Figure 3a). The absorption bands at 1399.93, 1239.72, 1210.46, 1144.81, and 1120.13 cm^{-1} are assigned to the C−F stretching vibration of the $-CF_2-$ and $-CF_3$ groups. Figure 3b shows the FTIR spectrum of the superhydrophobic Ti surface obtained via the same electrochemical etching method used to prepare the superoleophobic Ti surface. This surface was electrochemically etched for 10 min in the 0.2 mol L^{-1} NaBr solution at a 0.25 A/cm^2 current density and at 60−70 °C electrolyte temperature. After FAS modification, the surface became superhydrophobic. The absorption bands at 1146.38 and 1099.28 cm^{-1} are assigned to the C−F stretching vibration of the $-CF_2-$ and $-CF_3$ groups. These results indicate that the prepared superoleophobic or superhydrophobic Ti surfaces had been covered by the FAS film. Figure 3c shows the FTIR spectrum of the unprocessed Ti surface. No absorption peak appeared between 1400 and 1000 cm^{-1}, indicating the absence of the FAS film on the unprocessed Ti surface. Thus, the unprocessed Ti surface was neither hydrophobic nor oleophobic.

The elements on the Ti surfaces were detected via EDS. Figure 4a shows the EDS spectrum of the superoleophobic Ti surface. Aside from Ti, the elements of C, F, and O were also

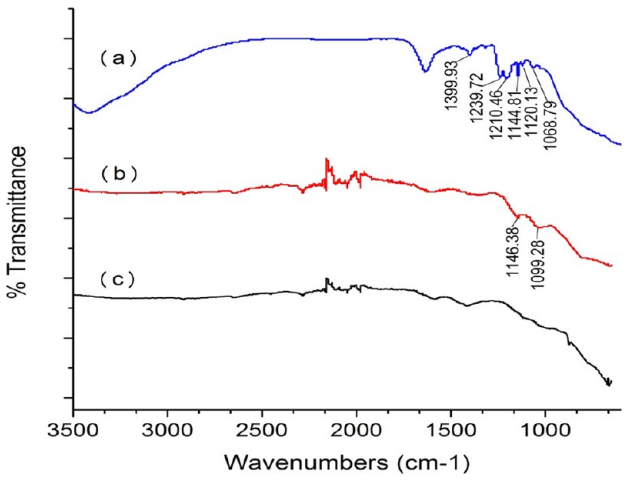

Figure 3. FTIR spectra of (a) superoleophobic Ti surface, (b) superhydrophobic Ti surface, and (c) unprocessed Ti surface.

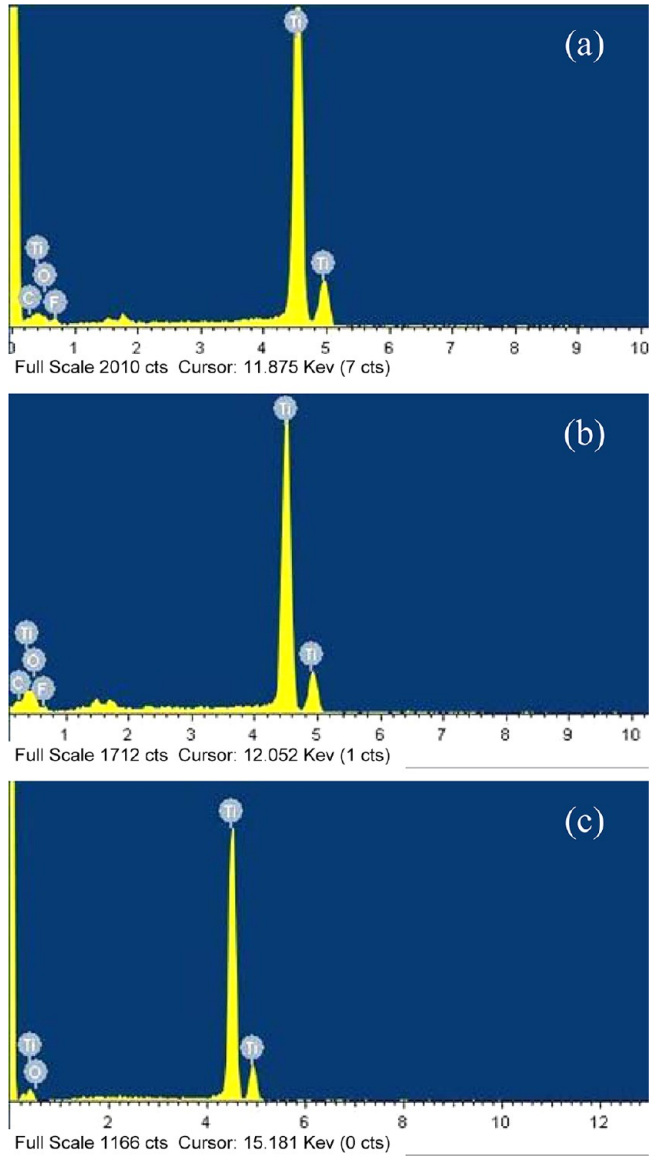

Figure 4. EDS spectra of (a) superoleophobic Ti surface, (b) superhydrophobic Ti surface, and (c) unprocessed Ti surface.

dx.doi.org/10.1021/sc3000527 | ACS Sustainable Chem. Eng. 2013, 1, 102−109

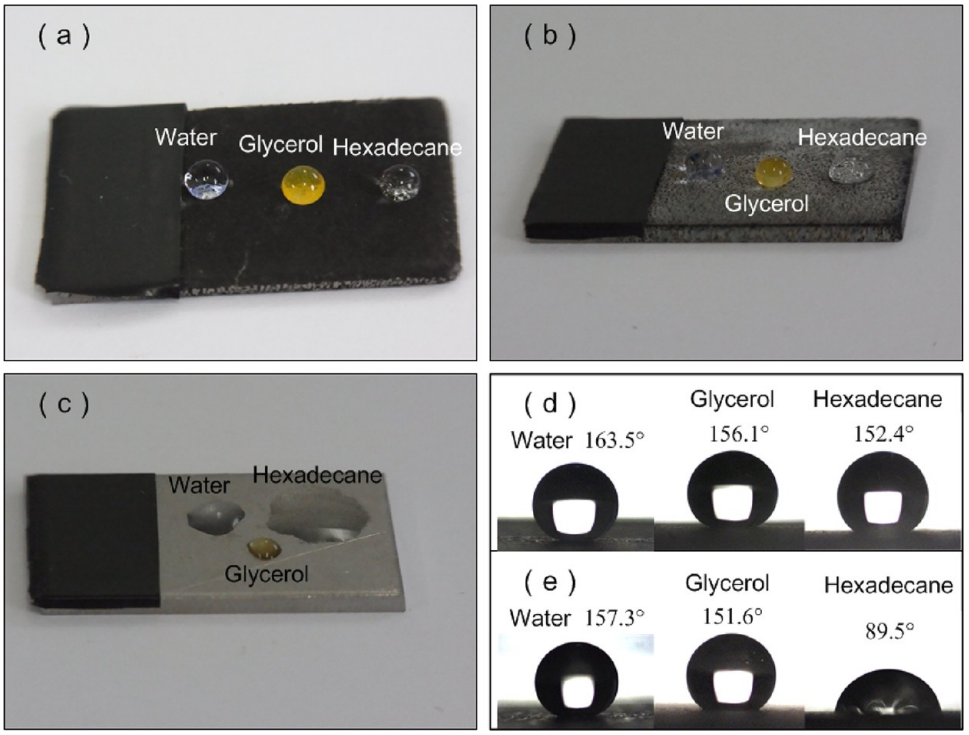

Figure 5. Images of (a) superoleophobic Ti surface, (b) superhydrophobic Ti surface, (c) unprocessed Ti surface, (d) superoleophobic Ti surface, and (e) superhydrophobic Ti surface. Values of contact angles are in (d) and (e).

found on the superoleophobic Ti surface. In a similar manner, the EDS spectrum of the superhydrophobic Ti surface shows the presence of Ti, C, F, and O (Figure 4b). Thus, Figure 4a,b confirms that the superoleophobic and superhydrophobic Ti surfaces were uniformly covered by the FAS film. Figure 4c shows the EDS spectrum of the unprocessed Ti surface. This surface consisted only of Ti and O. Therefore, the superoleophobic and superhydrophobic Ti surfaces were obtained via electrochemical etching and FAS modification.

Figure 5 shows the images of the superoleophobic Ti surface, the superhydrophobic Ti surface, and the unprocessed Ti surface. Water, glycerol, and hexadecane droplets remained on the superoleophobic Ti surface as spheres. This effect could be analyzed via the general wetting diagram as show in Figure 6,

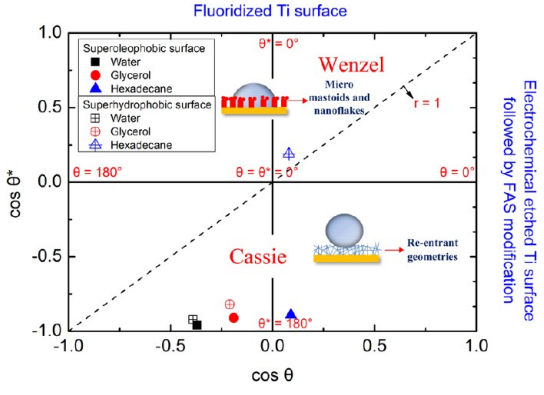

Figure 6. Plot of cos θ^* and cos θ for water, glycerol, and hexadecane on superoleophobic and superhydrophobic surfaces as a function of θ. θ is the liquid contact angle on a fluoridized Ti surface, and θ^* is the apparent liquid contact angle on superoleophobic and superhydrophobic surfaces.

which shows the plot of cos θ^* on rough electrochemical etched Ti surface as a function of cos θ for the comparatively smooth fluoridized Ti surface. These results are consistent with the Cassie and Baxter model. The re-entrant geometries allowed air to be trapped in the crevices and gaps of the microstructures under the liquid droplets, resulting in the formation of a heterogeneous surface. Air and the FAS film on this surface provided low surface energy, thus widening the contact angles of the re-entrant geometries and reducing the contact area of the liquid droplets with the surface. Therefore, superoleophobicity and superhydrophobicity depend on the synergistic effects of both surface structures and chemistry. Meanwhile, the water droplet remained spherical on the superhydrophobic Ti surface. Glycerol, a type of oil with a comparatively high surface tension (γ_g = 63.6 mN/m), could remain on the superhydrophobic Ti surface in a nearly spherical shape. However, hexadecane, a low surface tension liquid, stayed on this surface at a contact angle of <90°. Hexadecane droplets entered the crevices and gaps between the nanoflakes, which is in agreement with the Wenzel model as shown in Figure 6. The unprocessed surface, on which the three kinds of liquids were spread out, was both hydrophilic and oleophilic. Figure 5d,e shows clear images of the water, glycerol, and hexadecane droplets on the superoleophobic and superhydrophobic Ti surfaces, respectively.

Effects of Various Experimental Parameters. The effects of the current density, electrochemical etching time, electrolyte temperature, and electrolyte concentration on surface wettability for water, glycerol, and hexadecane were investigated in detail. Figure 7 shows the relationship of the current density with the contact angles and the rolling angles of water, glycerol, and hexadecane. The Ti surface was electrochemically etched for 10 min in the 0.2 mol L^{-1} NaBr solution at 60−70 °C electrolyte temperature. The current density

dx.doi.org/10.1021/sc3000527 | ACS Sustainable Chem. Eng. 2013, 1, 102−109

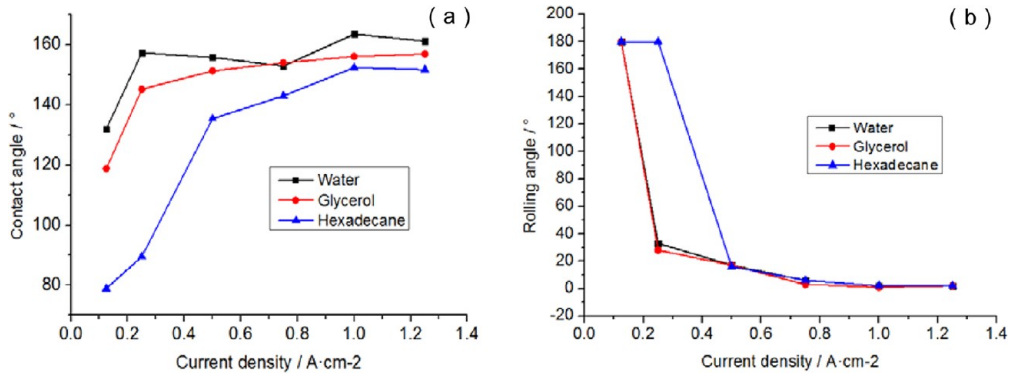

Figure 7. Relationship of the current density with (a) the contact angles and (b) the rolling angles of water, glycerol, and hexadecane.

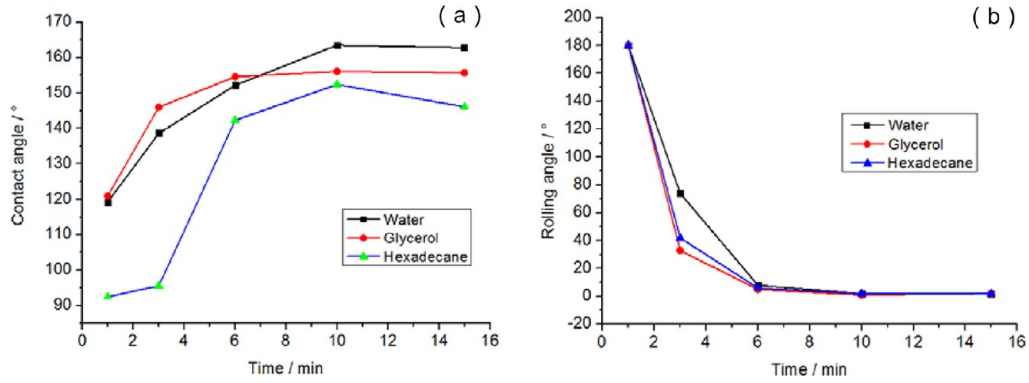

Figure 8. Relationship of the electrochemical etching time with (a) the contact angles and (b) the rolling angles of water, glycerol, and hexadecane.

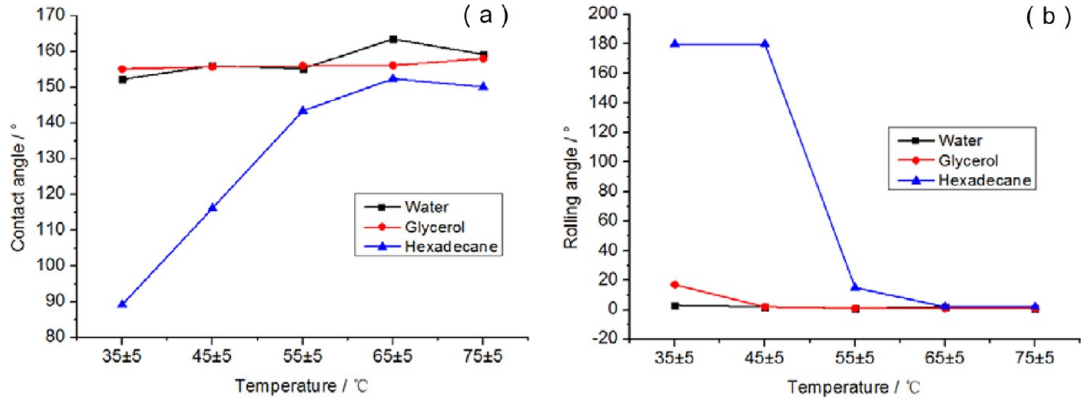

Figure 9. Relationship of the electrolyte temperature with (a) the contact angles and (b) the rolling angles of water, glycerol, and hexadecane.

ranged from 0.125 to 1.25 A/cm^2. As the current density increased, the contact angles of water, glycerol, and hexadecane showed an upward trend. When the current density increased, the electrochemical etching mass per unit time increased, which contributed to the formation of the rough micro/nanometer structures on the Ti surface. At the same current density, the water contact angle is generally larger than the glycerol contact angle, which is in turn larger than the hexadecane contact angle. At the 0.25 A/cm^2 current density, the water contact angle was >150°, whereas the hexadecane contact angle was <100°. Thus, the Ti surface treated at the 0.25 A/cm^2 current density was superhydrophobic. In terms of the rolling angles, the change trend of the water rolling angles with the current density is similar to that of the glycerol rolling angles. However, the hexadecane rolling angle at the 0.25 A/cm^2 current density was 180°, which is different from the water rolling angle. Meanwhile, the surface chemistry of the superhydrophobic Ti surface showed no difference with that of the superoleophobic surface according to the FTIR and EDS spectra (Figures 3 and 4, respectively). However, the surface morphologies of the superhydrophobic Ti surface (Figure 1d−f) and superoleophobic Ti surface (Figure 1a−c) showed significant differences. Therefore, the difference between the hydrophobic and oleophobic surfaces was only due to the surface morphologies.

Figure 8 shows the relationship of the electrochemical etching time with the contact angles and the rolling angles of water, glycerol, and hexadecane. The Ti surface was electrochemically etched in the 0.2 mol L^{-1} NaBr solution at a 1.0 A/cm^2 current density and at 60−70 °C electrolyte temperature. The electrochemical etching time was from 1 to 15 min. After 6 min etching, a superhydrophobic surface with a water contact

dx.doi.org/10.1021/sc3000527 | ACS Sustainable Chem. Eng. 2013, 1, 102−109

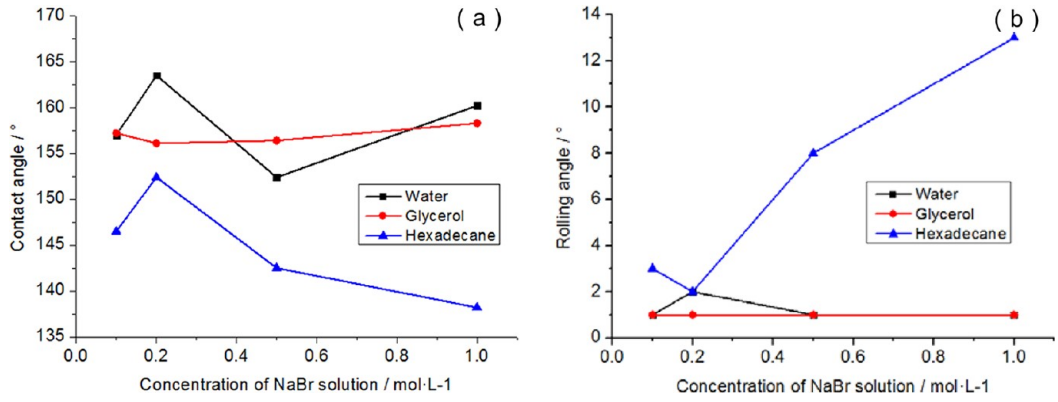

Figure 10. Relationship of the concentration of NaBr solution with (a) the contact angles and (b) the rolling angles of water, glycerol, and hexadecane.

angle greater than 150° was obtained. In addition, the rolling angles of water, glycerol, and hexadecane were <10°. When the electrochemical etching time was 10 min, the hexadecane contact angle was >150°, and a superoleophobic surface was obtained. The rolling angles of the three liquids were only 1−2°. The processing time had a negligible effect on wettability when the etching time exceeded 10 min. The electrochemical etching mass generally increases with increasing electrochemical etching time. In this study, the formation of rough micro/nanometer structures necessary for a superhydrophobic surface required 6 min. As the etching time was extended to 10 min, the electrochemical etching mass increased, the rough micro/nanometer structures became thinner, and re-entrant geometries were gradually formed. After FAS modification, the surface became superoleophobic.

Figure 9 shows the relationship of the electrolyte temperature with the contact angles and the rolling angles of water, glycerol, and hexadecane. The Ti surface was electrochemically etched for 10 min in the 0.2 mol L^{-1} NaBr solution at a 1.0 A/cm^2 current density. The electrolyte temperature profile was divided into 30−40, 40−50, 50−60, 60−70, and 70−80 °C. The electrolyte temperature significantly affected the wettability of hexadecane, which has a low surface tension, whereas the effects on water and glycerol, which have high surface tension, are negligible. As the electrolyte temperature increased, the hexadecane contact angle significantly increased. Beyond 50−60 °C, the hexadecane contact angle became relatively constant with some fluctuations at ∼150°. Meanwhile, the hexadecane rolling angles below 50 °C were 180°. Below 50−60 °C, the hexadecane rolling angle significantly decreased to ∼20°, before reaching 1−2°. This result is due to the passive nature of the Ti metal. As the electrolyte temperature increased, the activation energy of the electrolyte increased, whereas the open potential for the sacrificial anode decreased. The Ti oxidation film then became unstable and brittle. Without the protection of the Ti oxidation film, the crevices and gaps in smaller order would participate in reactions. Thus, the thinner and smaller re-entrant geometries on the Ti surface contributed to the superoleophobicity after FAS modification.

Figure 10 shows the relationship of the electrolyte concentration with the contact angles and the rolling angles of water, glycerol, and hexadecane. The Ti surface was electrochemically etched for 10 min at a 1.0 A/cm^2 current density and at 60−70 °C electrolyte temperature. The NaBr solution concentration ranged from 0.1 to 1.0 mol L^{-1}. The results indicate that the NaBr solution concentration exhibited the smallest effects on Ti surface wettability compared with the other experimental parameters. The 0.1 to 1.0 mol L^{-1} NaBr concentration resulted in contact and rolling angles of 135−165° and 1−13°, respectively, for the three liquids. The 10 min electrochemical etching was clearly sufficient for the formation of the surface rough micro/nanometer structures.[8] However, when the NaBr concentration exceeded 0.2 mol L^{-1}, the hexadecane contact angle decreased, whereas the hexadecane rolling angle increased. The re-entrant geometries increasingly became thinner and smaller than the nanoflakes, as the electrolyte concentration increased, eventually leading to the breakdown of such structures. However, as the re-entrant geometries dissolved, new re-entrant geometries were formed, thus retaining the dynamic equilibrium in a particular electrolyte concentration. This mechanism explains the negligible effect of the electrolyte concentration on the Ti surface wettability.

CONCLUSIONS

An economical and environmentally friendly electrochemical etching method was developed to prepare superoleophobic Ti surfaces with water, glycerol, and hexadecane contact angles greater than 150° and rolling angles of only 1−2°. Meanwhile, superhydrophobic surfaces were also prepared by adjusting the process parameters. Analysis of the neutral electrolyte, the reaction process, and the reaction products show that the proposed electrochemical method is economical and environmentally friendly. SEM images show that the re-entrant geometries are the key to achieving superoleophobicity and that the rough micro/nanometer structures are necessary to attain superhydrophobic surfaces. The XRD patterns show that the Ti surface crystal structures did not affect the hydrophobicity or oleophobicity of the Ti surface. FTIR and EDS spectra show that low surface energy materials are necessary to produce superhydrophobic and superoleophobic surfaces. Water, glycerol, and hexadecane droplets on superoleophobic surface are consistent with the Cassie and Baxter model, whereas a hexadecane droplet on a superhydrophobic surface is in agreement with the Wenzel model. The effects of electrochemical parameters such as the current density, electrochemical etching time, electrolyte temperature, and electrolyte concentration on the wettability for water, glycerol, and hexadecane were also investigated. The current density and electrochemical etching time both affected the hydrophobicity and oleophobicity. Temperature mainly affected the oleophobicity of the Ti surfaces. The NaBr solution concentration

dx.doi.org/10.1021/sc3000527 | ACS Sustainable Chem. Eng. 2013, 1, 102−109

exhibited the smallest effects among the parameters, affecting only the oleophobicity. The proposed method is believed to be adopted for industrial production of superoleophobic and superhydrophobic Ti surfaces for potential applications in various fields.

AUTHOR INFORMATION

Corresponding Author

*Tel.: + 86-411-84708422. Fax: + 86-411-84708422. E-mail address: wenjixu@dlut.edu.cn (W. Xu).

Notes

The authors declare no competing financial interest.

ACKNOWLEDGMENTS

The authors give thanks for the financial support from the National Natural Science Foundation of China (NSFC, Grant no. 90923022).

REFERENCES

(1) Barthlott, W.; Neinhuis, C. Purity of the sacred lotus, or escape from contamination in biological surfaces. *Planta* **1997**, *202*, 1−8.

(2) Neinhuis, C.; Barthlott, W. Characterization and distribution of water-repellent, self-cleaning plant surfaces. *Ann. Bot.* **1997**, *79*, 667−677.

(3) Gao, X.; Jiang, L. Biophysics: Water-repellent legs of water striders. *Nature* **2004**, *432*, 36.

(4) Tuteja, A.; Choi, W.; Ma, M.; Mabry, J. M.; Mazzella, S. A.; Rutledge, G. C.; McKinley, G. H.; Cohen, R. E. Designing superoleophobic surfaces. *Science* **2007**, *318*, 1618−1622.

(5) Liu, K.; Yao, X.; Jiang, L. Recent developments in bio-inspired special wettability. *Chem. Soc. Rev.* **2010**, *39*, 3240−3255.

(6) Wang, D.; Wang, X.; Liu, X.; Zhou, F. Engineering a titanium surface with controllable oleophobicity and switchable oil adhesion. *J. Phys. Chem. C* **2010**, *114*, 9938−9944.

(7) Tavana, H.; Amirfazli, A.; Neumann, A. W. Fabrication of superhydrophobic surfaces of *n*-hexatriacontane. *Langmuir* **2006**, *22*, 5556−5559.

(8) Parkin, I. P.; Palgrave, R. G. Self-cleaning coatings. *J. Mater. Chem.* **2005**, *15*, 1689−1695.

(9) Milne, A. J. B.; Amirfazli, A. Drop shedding by shear flow for hydrophilic to superhydrophobic surfaces. *Langmuir* **2009**, *25*, 14155−14164.

(10) Crick, C. R.; Parkin, I. P. Preparation and characterisation of super-hydrophobic surfaces. *Chem.—Eur. J.* **2010**, *16*, 3568−3588.

(11) Lu, Y.; Song, J.; Liu, X.; Xu, W.; Sun, J.; Xing, Y. Loading capacity of a self-assembled superhydrophobic boat array fabricated via electrochemical method. *Micro Nano Lett.* **2012**, *7*, 786−789.

(12) Jung, Y. C.; Bhushan, B. Dynamic effects of bouncing water droplets on superhydrophobic surfaces. *Langmuir* **2008**, *24*, 6262−6269.

(13) Kashaninejad, N.; Chan, W. K.; Nguyen, N. T. Eccentricity effect of micropatterned surface on contact angle. *Langmuir* **2012**, *28*, 4793−4799.

(14) Bhushan, B.; Koch, K.; Jung, Y. C. Nanostructures for superhydrophobicity and low adhesion. *Soft Matter* **2008**, *4*, 1799−1804.

(15) Yang, J.; Zhang, Z.; Xu, X.; Men, X.; Zhu, X.; Zhou, X. Superoleophobic textured aluminum surfaces. *New J. Chem.* **2011**, *35*, 2422−2426.

(16) Kim, H.; Noh, K.; Choi, C.; Khamwannah, J.; Villwock, D.; Jin, S. Extreme superomniphobicity of multiwalled 8 nm TiO_2 nanotubes. *Langmuir* **2011**, *27*, 10191−10196.

(17) Young, T. An essay on the cohesion of fluids. *Philos. Trans. R. Soc. London* **1805**, *95*, 65−87.

(18) Wenzel, R. N. Resistance of solid surfaces to wetting by water. *Ind. Eng. Chem.* **1936**, *28*, 988−994.

(19) Cassie, A. B. D.; Baxter, S. Wettability of porous surface. *Trans. Faraday Soc.* **1944**, *40*, 546−551.

(20) Tuteja, A.; Choi, W.; Mabry, J. M.; McKinley, G. H.; Cohen, R. E. Robust omniphobic surfaces. *Proc. Natl. Acad. Sci. U.S.A.* **2008**, *105*, 18200−18205.

(21) Tuteja, A.; Choi, W.; McKinley, G. H.; Cohen, R. E.; Rubner, M. F. Design parameters for superhydrophobicity and superoleophobicity. *MRS Bull.* **2008**, *33*, 752−758.

(22) Bellanger, H.; Darmanin, T.; Guittard, F. Surface structuration (micro and/or nano) governed by the fluorinated tail lengths toward superoleophobic surfaces. *Langmuir* **2012**, *28*, 186−192.

(23) Darmanin, T.; Guittard, F. Molecular design of conductive polymers to modulate superoleophobic properties. *J. Am. Chem. Soc.* **2009**, *131*, 7928−7933.

(24) Tian, Y.; Liu, H.; Deng, Z. Electrochemical growth of gold pyramidal nanostructures: Toward super-amphiphobic surfaces. *Chem. Mater.* **2006**, *18*, 5820−5822.

(25) Lu, X.; Leng, Y. Electrochemical micromachining of titanium surfaces for biomedical applications. *J. Mater. Process. Technol.* **2005**, *169*, 173−178.

(26) Su, Y. W.; Ji, B. H.; Zhang, K.; Gao, H. J.; Huang, Y. G.; Hwang, K. Nano to micro structural hierarchy is crucial for stable superhydrophobic and water-repellent surfaces. *Langmuir* **2010**, *26*, 4984−4989.

(27) Kelly, E. J. *Electrochemical Behavior of Titanium*; Bockrio, J. O., Conway, B. E., White, R. E., Eds.; Plenum Press: New York, 1982.

(28) Noë1, J. J. Ph.D. Thesis, University of Manitoba Winnipeg, Manitoba, Canada, 1999.